Liquid Crystals
Publication details, including instructions for authors and subscription information:
http://www.informaworld.com/smpp/title~content=t713926090

Dielectric studies of a laterally-linked siloxane ester dimer

Sergio Diez; David A. Dunmur Corresponding author[a]; M. Rosario De La Fuente; Panagiota K. Karahaliou[b]; Georg Mehl[c]; Thomas Meyer[c]; Miguel Ángel PerÉz Jubindo; Demetri J. Photinos[b]
[a] Department of Chemistry and Southampton Liquid Crystal Institute, University of Southampton, Southampton SO17 1BJ, United Kingdom [b] Department of Materials Science, University of Patras, Patras 26500, Greece [c] Department of Chemistry, University of Hull, Hull HU6 7RX, United Kingdom

Online publication date: 19 May 2010

To cite this Article Diez, Sergio , Dunmur Corresponding author, David A. , De La Fuente, M. Rosario , Karahaliou, Panagiota K. , Mehl, Georg , Meyer, Thomas , Jubindo, Miguel Ángel PerÉz and Photinos, Demetri J.(2003) 'Dielectric studies of a laterally-linked siloxane ester dimer', Liquid Crystals, 30: 9, 1021 — 1030
To link to this Article: DOI: 10.1080/0267829031000152969
URL: http://dx.doi.org/10.1080/0267829031000152969

LIQUID CRYSTALS, VOL. 30, NO. 9, SEPTEMBER, 2003, 1021–1030

Taylor & Francis
Taylor & Francis Group

Dielectric studies of a laterally-linked siloxane ester dimer

SERGIO DIEZ, DAVID A. DUNMUR*†, M. ROSARIO DE LA FUENTE, PANAGIOTA K. KARAHALIOU‡, GEORG MEHL§, THOMAS MEYER§, MIGUEL ÁNGEL PERÉZ JUBINDO and DEMETRI J. PHOTINOS‡

Departamento de Fisica Aplicada II, Facultad de Ciencias, Universidad del Pais Vasco, Apdo. 644, 48080 Bilbao, Spain
†Department of Chemistry and Southampton Liquid Crystal Institute, University of Southampton, Southampton SO17 1BJ, United Kingdom
‡Department of Materials Science, University of Patras, Patras 26500, Greece
§Department of Chemistry, University of Hull, Hull HU6 7RX, United Kingdom

(*Received 29 January 2003; accepted 20 April 2003*)

This paper reports measurements of the dielectric response over the frequency range 10^2 to 10^9 Hz of a liquid crystal dimer consisting of two ester mesogens laterally linked by an alkoxy chain containing a siloxane group. The synthesis and phase behaviour of the siloxane dimer are also reported. Results show that there are two relaxations in the isotropic phase and four in the nematic phase of the material. The possible molecular origins for these modes are given. It is found that there is a coupling between internal and external modes which gives rise to a cooperative mode as the temperature in the nematic phase is lowered towards a glass transition.

1. Introduction

Anisometric rigid molecules can form lyotropic and thermotropic mesophases, but the attachment of flexible groups to the molecules can often enhance their mesophase behaviour. Attached alkyl chains promote fluidity through a reduction of symmetry and a lowering of the crystallization temperatures. Alkyl chains are the most common flexible group used in the design and synthesis of liquid crystalline compounds, but others such as the siloxane group have been successfully used [1]. The siloxane group is of special interest since it is well known that it promotes wide isotropic liquid ranges. The increased fluidity imparted to mesogens by siloxane groups can also promote wider ranges of temperature for the corresponding mesophases. Another consequence of the introduction of alkyl or siloxane chains, or indeed any chemically distinct groups, is that of microphase separation. Thus at a molecular level there is a tendency for groups of similar chemical type to associate giving rise to a local molecular organization, which may propagate over macroscopic distances to give new phase types. The microphase separation of hydrophilic and hydrophobic groups is familiar in micelle formation and lyotropic liquid crystals. In these and related mesophases, the flexible alkyl chains are segregated from the rigid parts of the mesogen, giving rise to structurally modulated mesophases. This also happens with other flexible or semiflexible groups such as siloxane or perfluoro chains attached to mesogens [2]. Another aspect of flexibility in mesogens that will be of interest to us in this paper, is the use of flexible groups to change molecular shape.

The shape of the constituent molecules in liquid crystals is a vital factor in determining the mesophase properties, hence our categorization of molecules as, for example, rod-like, disc-like, banana- or V-shaped. For rigid mesogens, control over molecular shape is through molecular design, but flexibility provides an internal mechanism to change the molecular shape, and so in principle is another design concept. However in this case the molecular shape changes are determined by influences such as changes in conformational distributions due to temperature, intermolecular interactions and external fields. While direct control of these effects is not usually possible, the property changes that result from changes of molecular shape can be very large; they can occur very rapidly, and may be subject to local feed-back mechanisms which can enhance or moderate their influence.

Connecting two mesogenic groups by a flexible linking group results in so-called liquid crystal dimers [3]. The mesogenic groups may be identical, giving symmetric dimers, or different, resulting in non-symmetric dimers. The different possibilities for the mutual orientation of the mesogenic groups define the range of molecular shapes available to the liquid crystal dimer,

*Author for correspondence; e-mail: d.a.dunmur@soton.ac.uk

Liquid Crystals ISSN 0267-8292 print/ISSN 1366-5855 online © 2003 Taylor & Francis Ltd
http://www.tandf.co.uk/journals
DOI: 10.1080/0267829031000152969

and hence determine the corresponding mesophase properties. The dimers we used for earlier dielectric studies were those in which the two mesogenic groups were attached longitudinally to the flexible linking chain. However the mesogenic groups may be attached in a variety of configurations to the chain, and in this paper we consider a material in which the mesogenic groups are laterally attached to the flexible chain. The particular material studied was a siloxane-linked dimer having different mesogenic groups laterally attached at each end of a thirteen-member chain. The compound used in this study was prepared as a precursor in the construction of dendrimeric liquid crystals [4] having a variety of siloxane cores.

Previous studies of the dielectric properties of longitudinally linked dimers have been reported [5], and a qualitative model has been proposed to explain the experimental observations. The basis of this model is the change in conformational distribution caused by temperature, and the corresponding changes in the degree of orientational order of the mesogenic groups. Using the RIS model for the conformational distribution of alkyl chains, it has already been shown [6–8] that the distribution function for the angle between terminal groups can be realistically approximated by a bimodal distribution in both the isotropic and nematic phases. Thus for an even-membered chain, the end groups tend to be either anti-parallel, or make an angle of about 71° (180° minus the tetrahedral angle); while for odd-membered chains the end groups are either parallel or at an angle of about 109° (the tetrahedral angle). These results suggest that as a first approximation to a model for the angular distribution of the terminal groups of liquid crystal dimers, it is acceptable to use a two-state model for either odd or even dimers. The model satisfactorily explains the results previously reported on the dielectric properties of both symmetric and non-symmetric dimers, in which the end mesogenic groups are longitudinally attached to the flexible chain.

The longitudinal dimers already reported are synthesized by connecting the mesogenic groups to the flexible chain in such a manner that the axes of the mesogen and the extended chain are, as far as possible, parallel. It is possible to connect the mesogenic groups to the flexible chain at other positions. In lateral dimers the mesogenic groups are connected such that the axes of anisometric groups are approximately perpendicular to the axis of the extended chain. In this paper we report dielectric measurements for a laterally connected liquid crystalline dimer, the flexible chain in which has a centrally placed disiloxane unit. The results indicate that the flexible chain allows the contribution of different conformers to the dielectric relaxation.

2. Materials

The siloxane-coupled dimer **10** was prepared according to the reaction scheme given below. Alkylation of methyl 2,4-dihydroxybenzoate **1** with bromo-octane firstly in the *p*-position of the aromatic ring and subsequently with 5-bromo-1-pentene in the *o*-position in a Williamson etherification, followed by removal of the methyl group protecting the carboxylic acid function leads to the intermediate **4**. Compound **7** containing four aromatic rings was obtained by esterification of **4** with **5**, the product of the esterification of octyloxybenzoic acid with 4,4′-biphenol. Esterification of the intermediate **4** with 4-hydroxy-4′-undecyloxybiphenyl **6** yields the compound **8** containing three aromatic rings. Compound **8** is converted via hydrosilylation with 1,1,3,3-tetramethyldisiloxane and Karstedt's catalyst to compound **9**, which is subsequently reacted with compound **7** in toluene to yield the mixed dimer **10**. Details of typical preparations are given below. The purified material exhibited a wide nematic range, which could be readily supercooled. Transition temperatures were obtained from optical microscopy and DSC. The observed phase behaviour was: isotropic – 106°C – nematic – −9°C – glass. It is a feature of laterally connected dimers that nematic phases tend to be stabilized, and smectic phases destabilized. The observation of a glass transition rather than crystallization is almost certainly a consequence of the presence of a siloxane group in the linking chain. The enhanced flexibility of this linkage tends to prevent crystallization.

2.1. *Methyl 2-hydroxy-4-octyloxybenzoate (**2**)*

A solution of bromooctane (63 ml, 0.36 mol) in dry butanone (200 ml) was added under reflux to a suspension of methyl 2,4-dihydroxybenzoate (51.0 g, 0.30 mol), K_2CO_3 (207 g, 1.5 mol) and powdered 4 Å molecular sieves (60 g) in dry butanone (1000 ml) over a 7 h period. The reaction mixture was heated under reflux for an additional 18 h until the reaction was complete (TLC). After filtration of the reaction mixture the butanone was distilled off and the residue recrystallized three times from methanol (100 ml) to yield white crystals; 74.5 g, 0.27 mol, 88%, m.p. 46–47°C, $R_f(CH_2Cl_2) = 0.63$. Anal: calcd for $C_{16}H_{24}O_4$ (280.36) C 68.55, H 8.63; found C 68.85, H 8.90%. ^{1}H NMR (270 MHz, $CDCl_3$): $\delta = 0.89$ (t, 3 H, CH_3), 1.25–1.48 (m, 10 H, CH_2), 1.74–1.81 (m, 2 H, OCH_2CH_2), 3.91 (s, 3 H, OCH_3), 3.96 (t, 2 H, OCH_2), 6.41–6.43 (m, 2 H, CH_{arom}), 7.70–7.30 (m, 1 H, CH_{arom}), 11.00 (s, 1 H, OH).

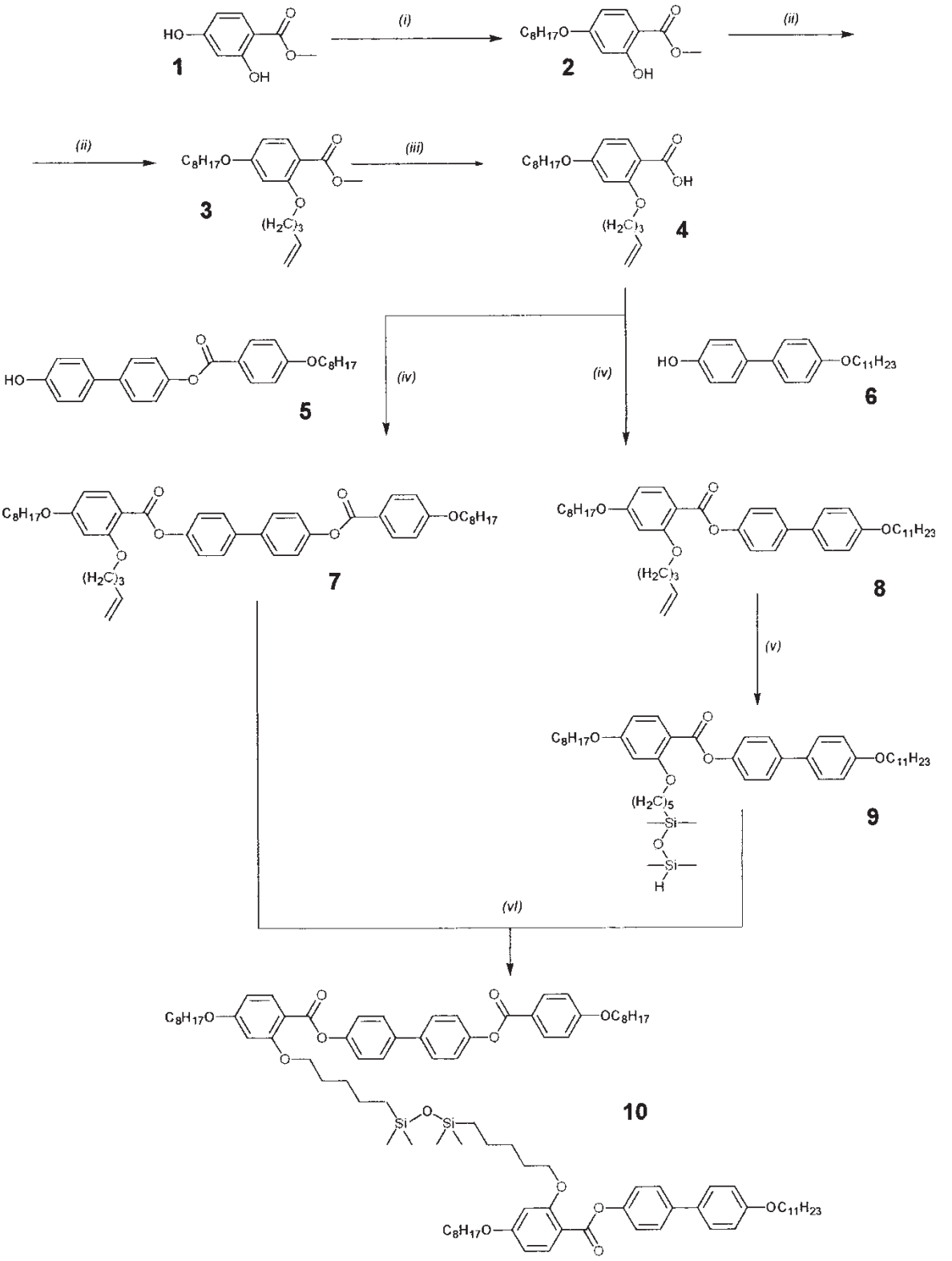

Scheme. (i) K_2CO_3, KI, 4 Å molecular sieves, butanone, bromo-octane, ΔT, 88%; (ii) K_2CO_3, KI, 4 Å molecular sieves, butanone, 5-bromo-1-pentene, ΔT, 95%; (iii) 1) NaOH, H_2O, MeOH, THF, 2) HCl, H_2O, 90%; (iv) 1) $SOCl_2$, toluene, ΔT, 2) pyridine, toluene, ΔT, 85%; (v) 1,1,3,3-tetramethyldisiloxane, toluene, Karstedt's catalyst, r.t., 80%; (vi) toluene, Karstedt's catalyst, r.t., 65%.

2.2. *Methyl 4-octyloxy-2-(pent-4-en-1-yloxy)benzoate (**3**)*

Bromopent-4-ene (44.7 g, 0.30 mol) was added to a suspension of compound (**2**) (66.1 g, 0.234 mol), K_2CO_3 (207 g, 1.5 mol), KI (5.0 g, 0.03 mol) and powdered 4 Å molecular sieves (50 g) in dry butanone (700 ml), and the mixture was heated under reflux until the reaction was complete (approx. 8 days). The reaction mixture was filtered and the butanone distilled off. After drying the residue in vacuum a slightly yellow oil (77.5 g, 0.22 mol, 95%) was obtained, which could be used in the next reaction without further purification. $R_f(CH_2Cl_2) = 0.51$. ^{1}H NMR (270 MHz, $CDCl_3$): $\delta = 0.87$–0.90 (m, 3 H, CH_3), 1.25–1.48 (m, 10 H, CH_2), 1.74–1.81 (m, 2 H, OCH_2), 1.90–1.97 (m, 2 H, OCH_2), 2.26–2.32 (m, 2 H, $CH_2CH=CH_2$), 3.85 (s, 3 H, OCH_3), 3.96–4.03 (m, 4 H, OCH_2), 4.97–5.09 (m, 2 H, CH–CH_2), 5.81–5.91 (m, 1 H, $CH=CH_2$), 6.45–6.48 (m, 2 H, CH_{arom}), 7.82–7.84 (m, 1 H, CH_{arom})

2.3. *4-Octyloxy-2-(pent-4-en-1-yloxy)benzoic acid (**4**)*

Compound **3** (77.5 g, 0.22 mol) was dissolved in THF (250 ml) and methanol (1400 ml). A solution of KOH (66.6 g, 1.19 mol) in water (200 ml) was added. After stirring for 2 days at r.t. the reaction was completed by heating at reflux for 2 h. The solvents were distilled off and ice/water (900 ml) added. After acidification with conc. HCl (110 ml) the mixture was extracted with CH_2Cl_2 (6×250 ml). After drying the CH_2Cl_2 phase with $MgSO_4$ the solvent was distilled off. Recrystallization from hexane yielded off-white crystals; 66.9 g, 0.20 mol, 92%, m.p. 67–68°C, $R_f(CH_2Cl_2) = 0.60$. Anal: calcd for $C_{20}H_{30}O_4$ (334.45) C 71.83, H 9.04; found C 72.99, H 9.65%. ^{1}H NMR (270 MHz, $CDCl_3$): $\delta = 0.89$ (t, 3 H, CH_3), 1.25–1.49 (m, 10 H, CH_2), 1.76–1.83 (m, 2 H, OCH_2), 1.99–2.05 (m, 2 H, OCH_2), 2.24–2.29 (m, 2 H, $CH_2CH=CH_2$), 4.01 (t, 2 H, OCH_2), 4.21–4.24 (t, 2 H, OCH_2), 5.05–5.12 (m, 2H, $CH=CH_2$), 5.78–5.88 (m, 1 H, $CH=CH_2$), 6.51 (d, 1 H, CH_{arom}), 6.61–6.64 (dd, 1 H, CH_{arom}), 8.12 (d, 1 H, CH_{arom}), 10.72 (br, 1 H, COOH).

2.4. *4′-Hydroxy-biphenyl-4-yl 4-octyloxybenzoate (**5**)*

4-Octyloxybenzoic acid (45.0 g, 0.18 mol), 4,4′-dihydroxybiphenyl (70.0 g, 0.38 mol) and *N*,*N*-dimethylaminopyridine (4.60 g, 37.7 mmol) were dissolved in dry THF (1000 ml) and *N*,*N*′-cyclohexylcarbodiimide (44.0 g, 0.21 mol) was added. After stirring for 18 h at r.t. the reaction mixture was filtered, the filtrate washed with CH_2Cl_2 and the solvents distilled off. The residue was dissolved in hot ethanol under reflux and after cooling to r.t. the suspension was filtered. The residue was dissolved in a hot solution of hexane/$CHCl_3$/THF = 2/2/1 and after cooling to r.t. the residue was filtered off. The recrystallization was repeated until the TLC indicated a pure (white) product **5**; 37.2 g, 88.9 mmol, 49%, m.p. 183°C, $R_f(CH_2Cl_2) = 0.43$. Anal: calcd for $C_{27}H_{30}O_4$ (418.53) C 77.48, H 7.22; found C 77.19, H 7.37%. ^{1}H NMR (270 MHz, CD_2Cl_2/d_6-DMSO = 1/1): $\delta = 0.87$ (t, 3 H, CH_3), 1.27–1.49 (m, 10 H, CH_2), 1.73–1.84 (m, 2 H, OCH_2CH_2), 4.03 (t, 2 H, OCH_2), 6.86–6.89 (m, 2 H, CH_{arom}), 6.96–6.98 (m, 2 H, CH_{arom}), 7.18–7.20 (m, 2 H, CH_{arom}), 7.41–7.43 (m, 2 H, CH_{arom}), 7.54–7.56 (m, 2 H, CH_{arom}), 8.09–8.11 (m, 2 H, CH_{arom}), 8.95 (br, 1 H, OH).

2.5. *4-Hydroxy-4′-undecyloxybiphenyl (**6**)*

Sodium metal (17.2 g, 0.72 mol) was dissolved in dry methanol (600 ml) with exclusion of moisture and 4,4′-dihydroxy biphenyl (50.6 g, 0.72 mol) added. Bromoundecane (57.8 ml,) was added dropwise to this solution and after adding KI (4.6 g) the reaction mixture was heated at reflux for 20 h. After cooling to r.t. a solution of NH_4Cl (20 g) in water (500 ml) was added. The product was filtered off, washed with water (100 ml) and methanol (100 ml). Repeated recrystallization from butanone (800 ml) yielded a beige powder; 39.8 g, 0.117 mol, 43%, m.p. 148–149°C. Anal: calcd for $C_{23}H_{32}O_2$ (340.50) C 81.13, H 9.47; found C 81.36, H 9.81%. ^{1}H NMR (270 MHz, $CDCl_3$/d_6-DMSO = 1/1): $\delta = 0.88$ (t, 3 H, CH_3), 1.24–1.50 (m, 16 H, CH_2), 1.74–1.81 (m, 2 H, OCH_2CH_2), 3.97 (t, 2 H, OCH_2), 6.85–6.87 (m, 2 H, CH_{arom}), 6.89–6.92 (m, 2 H, CH_{arom}), 7.34–7.37 (m, 2 H, CH_{arom}), 7.40–7.44 (m, 2 H, CH_{arom}), 9.00 (s, 1 H, OH).

2.6. *4′-(4-Octyloxybenzoyloxy)biphenyl-4-yl 4-octyloxy-2-(pent-4-en-1-yloxy)benzoate (**7**)*

Compound **4** (5.36 g, 16.0 mmol) was dissolved in dry toluene (65 ml) under nitrogen; thionylchloride (25 ml, 0.34 mol) was added and the solution heated to 80°C for 2 h, with a final reflux for an additional hour. After cooling to r.t. the thionylchloride and toluene was distilled off under nitrogen. The residue was dissolved in toluene (40 ml) and a solution of compound **5** (6.70 g, 16.0 mmol) and dry pyridine (25 ml, 0.31 mol) in toluene (25 ml) added dropwise over 5 min. The solution was heated to 80°C for 18 h and after refluxing for an additional hour was cooled to r.t. Saturated aqueous NaCl (120 ml) and diethyl ether (120 ml) was then added. After phase separation the aqueous layer was extracted with $CHCl_3$/hexane = 1/1 (3×120 ml). The organic layers were combined and dried with $MgSO_4$; the solvents were then distilled off and the residue purified by column chromatography (silica gel, CH_2Cl_2/hexane = 4/1). Recrystallization from hexane yielded a white solid product; 10.0 g, 13.7 mmol, 85%,

m.p. 89°C. Anal: calcd for $C_{47}H_{58}O_7$ (734.97) C 76.81, H 7.95; found C 76.58, H 7.83%. ^{1}H NMR (270 MHz, $CDCl_3$): $\delta = 0.80$–0.85 (m, 6 H, CH_3), 1.23–1.50 (m, 20 H, CH_2), 1.70–1.78 (m, 4 H, OCH_2CH_2), 1.83–1.90 (m, 2 H, OCH_2CH_2), 2.20–2.25 (m, 2 H, $CH_2CH=CH_2$), 3.94–3.99 (m, 6 H, OCH_2), 4.88–4.97 (m, 2 H, $CH_2CH=CH_2$), 5.70–5.81 (m, 1 H, $CH_2CH=CH_2$), 6.43–6.48 (m, 2 H, CH_{arom}), 6.90–6.95 (m, 2 H, CH_{arom}), 7.15–7.25 (m, 4 H, CH_{arom}), 7.52–7.57 (m, 4 H, CH_{arom}), 7.98 (d, 1 H, CH_{arom}), 8.08–8.12 (m, 2 H, CH_{arom}).

2.7. *4′-Undecyloxybiphenyl-4-yl 4-octyloxy-2-(pent-4-en-1-yloxy)benzoate (**8**)*

Compound **4** (10.6 g, 31.7 mmol) was dissolved in dry toluene (130 ml) under nitrogen; thionyl chloride (50 ml, 0.68 mol) was added and the solution heated to 80°C for 3 h, the reaction being completed after heating for 45 min at reflux. The thionyl chloride and toluene were distilled off under nitrogen. A solution of compound **6** (10.8 g, 31.7 mmol) and pyridine (50 ml, 0.62 mol) in toluene (50 ml) was added to the residue. This reaction mixture was heated at 80°C for 18 h and the reaction completed after reflux for 1 h. Ice–water (400 ml) and 1/1 ether/hexane (400 ml) was then added; the phases were separated and the organic layer extracted with $CHCl_3$ (2 × 250 ml). The combined organic layers were dried with $MgSO_4$ and the solvents distilled off. The residue was purified by column chromatography (silica gel, CH_2Cl_2/hexane = 4/1). Recrystallization from hexane yielded a white product; 16.6 g, 25.3 mmol, 80%, m.p. 72°C. Anal: calculated for $C_{43}H_{60}O_5$ (656.95) C 78.62, H 9.21; found C 78.59, H 9.45. ^{1}H NMR (270 MHz, $CDCl_3$): $\delta = 0.87$–0.91 (m, 6 H, CH_3), 1.23–1.46 (m, 26 H, CH_2), 1.76–1.84 (m, 4 H, OCH_2CH_2), 1.91–1.98 (m, 2 H, OCH_2CH_2), 2.26–2.32 (m, 2 H, $CH_2CH=CH_2$), 3.97–4.07 (m, 6 H, OCH_2), 4.94–5.05 (m, 2 H, $CH_2CH=CH_2$), 5.77–5.87 (m, 1 H, $CH_2CH=CH_2$), 6.48–6.56 (m, 2 H, CH_{arom}), 6.94–6.98 (m, 2 H, CH_{arom}), 7.20–7.25 (m, 2 H, CH_{arom}), 7.48–7.58 (m, 4 H, CH_{arom}), 8.04 (d, 1 H, CH_{arom}).

2.8. *4′-Undecyloxy-biphenyl-4-yl 4-octyloxy-2-[5-(1,1,3,3-tetramethyldisiloxanyl)-pent-1-yloxylbenzoate (**9**)*

Compound **8** (4.06 g, 6.18 mmol) was dissolved in dry toluene (70 ml) and 1,1,3,3-tetramethyldisiloxane (52 ml, 0.29 mol) added. Dry air was bubbled through the solution for 2 min and a solution of platinium(0)-1,3-divinyl-1,1,3,3-tetramethyldisiloxane complex in xylene (5%, approx. 80 µl) was added. After stirring at r.t. for 20 h with exclusion of moisture, the solvent and excess of 1,1,3,3-tetramethyldisiloxane was distilled off under vacuum. The residue was purified by column chromatography (silica gel, CH_2Cl_2/hexane = 2/1) to yield a slightly yellow oil; 3.67 g, 4.64 mmol, 75%, $R_f(CH_2Cl_2$/hexane = 1/1) = 0.44. $C_{47}H_{74}O_6Si_2$ (791.26), ^{1}H NMR (270 MHz, $CDCl_3$): $\delta = 0.05$ (s, 6 H, $SiCH_3$), 0.15 (d, 6 H, $SiCH_3$), 0.53–0.59 (m, 2 H, $SiCH_2$), 0.88–0.93 (m, 6 H, CH_3), 1.29–1.58 (m, 30 H, CH_2), 1.78–1.87 (m, 6 H, OCH_2CH_2), 3.99–4.07 (m, 6 H, OCH_2), 4.65–4.68 (m, ≈1H, SiH), 6.52–6.58 (m, 2 H, CH_{arom}), 6.95–6.98 (m, 2 H, CH_{arom}), 7.21–7.25 (m, 2 H, CH_{arom}), 7.52–7.63 (m, 4 H, CH_{arom}), 7.99–8.00 (m, 1 H, CH_{arom}).

2.9. *Compound **10***

Compound **7** (500 mg, 0.68 mmol) and freshly prepared compound **9** (540 mg, 0.68 mmol) were dissolved in dry toluene (20 ml) and dry air bubbled through the solution for 2 min. A solution of platinium(0)-1,3-divinyl-1,1,3,3-tetramethyldisiloxane complex in xylene (5%, approx. 30 µl) was added. After stirring for 20 h with exclusion of moisture, the solvent was evaporated under vacuum. The residue was purified by column chromatography (silica gel, 2 × 30 cm, 1/1-dichloromethane/hexane). Recrystallization from hexane yielded the product as a white powder; 675 mg, 0.44 mmol, 65%. Anal: calcd for $C_{94}H_{132}O_{13}Si_2$ (1526.23) C 73.98, H 8.72; found C 74.29, H 8.96%. ^{1}H NMR ($CDCl_3$, 400 MHz): 0.00 (s, 6 H, $SiCH_3$), 0.47–0.51 (m, 4 H, $SiCH_2$), 0.81–0.90 (m, 12 H, CH_3), 1.25–1.34 (m, 30 H, CH_2), 1.40–1.54 (m, 16 H, CH_2), 1.75–1.89 (m, 12 H, OCH_2CH_2), 3.95–4.07 (m, 12 H, OCH_2), 6.50–6.52 (m, 4 H, =CH), 6.94–7.00 (m, 4 H, =CH), 7.20–7.28 (m, 6 H, =CH), 7.45–7.63 (m, 8 H, =CH), 8.01–8.08 (m, 2 H, =CH), 8.15–8.17 (m, 2 H, =CH). ^{13}C NMR ($CDCl_3$, 400 MHz): 164.92, 164.42, 164.37, 164.09, 164.00, 163.52, 161.67, 161.64, 158.62, 150.67, 150.44, 150.10, 138.19, 138.17, 137.73, 134.36, 132.90, 132.26, 128.08, 128.02, 127.53, 122.28, 122.13, 122.04, 121.45, 114.71, 114.26, 111.22, 111.12, 105.22, 100.15, 68.87, 68.28, 68.02, 31.87, 31.77, 29.59, 29.55, 29.38, 29.30, 29.27, 29.19, 29.10, 29.06, 28.84, 26.03, 25.95, 23.00, 22.65, 22.61, 18.23, 14.07, 0.32, ^{29}Si-Dept-NMR ($CDCl_3$, 400 MHz): 7.84.

3. Dielectric measurements

The dielectric permittivity of the material was measured over the temperature range −10 to 110°C and over the frequency range 10^2 to 10^9 Hz using two impedance analysers: HP4192A (10^2 to 10^7 Hz) and HP4291A (10^6 to 10^9 Hz). For the measurements, cells with gold plated electrodes (separation 50 µm) were used, but without any surface treatment. Under such circumstances, most materials spontaneously align such that the director is in the plane of the electrode surfaces. It is possible to apply a bias voltage, up to

35 V, which causes materials of positive dielectric anisotropy to align with their directors perpendicular to the electrode surfaces. The material studied in this work had a negative dielectric anisotropy, so application of a bias electric field stabilized the planar alignment. At low frequencies it was possible to use ITO-coated glass cells (EHC, Japan), having a sample thickness of 25 μm. Cells having surface treatment for planar or homeotropic alignments were available. The negative dielectric anisotropy of the material was established by observing the behaviour of ITO-coated glass cells with a planar aligned sample when a bias voltage was applied. Above a critical voltage, patterns of electrohydrodynamic instabilities developed, which are characteristic of a material having a negative dielectric anisotropy and a positive conductivity anisotropy [9].

4. Results

Measurements of the real and imaginary parts of the permittivity in the isotropic phase at 108°C are presented in figure 1. The experimental points are plotted, as is the fit to equation (1) below:

$$\varepsilon(\omega) = \sum_k \Delta\varepsilon_k(\omega) + \varepsilon_\infty - \mathrm{i}\sigma_{\mathrm{dc}}/\omega\varepsilon_0 \qquad (1)$$

where σ_{dc} is the d.c. conductivity and ε_∞ is the high frequency permittivity. Equation (1) represents the complex dielectric response as a sum over separate relaxation modes k, each of which can be characterized by a function, $\Delta\varepsilon_k$ (ω), which can be fitted to the Havriliak–Negami function:

$$\Delta\varepsilon_k(\omega) = \frac{\Delta\varepsilon_k}{[1+(\mathrm{i}\omega\tau_k)^{\alpha_k}]^{\beta_k}} \qquad (2)$$

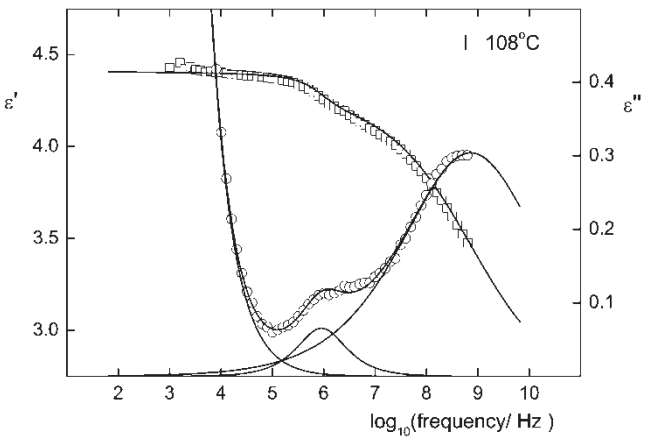

Figure 1. Complex dielectric permittivity vs logarithm of the frequency at 108°C in the isotropic phase: □ real component; ○ imaginary component. The solid lines give the best fit to equation (1) with two modes.

where $\Delta\varepsilon_k$ is the strength of each mode. τ_{k} is related to the inverse frequency of maximum dielectric losses for each mode, and α_{k} and β_{k} are parameters which describe the shape of the relaxation spectra: $\alpha=\beta=1$ corresponds to a simple Debye-type relaxation. The real and imaginary components of the measured permittivity were fitted simultaneously to equations (1) and (2), and we obtained for each temperature the strength and frequency of the dielectrically active relaxational modes. An alternative method of obtaining the relaxation frequencies from a derivative plot of the real part of the permittivity has recently been reported [10], which works well for materials of high dielectric constant. For the material reported here, the relatively small dielectric strengths of some modes at some temperatures makes the derivative plot method less reliable than fitting over the full frequency range.

It is clear that after allowance for the d.c. conductivity, there are two separated relaxations in the isotropic phase, that at the higher frequency being more intense. Given the rather complex structure of the mesogen, it is perhaps surprising that the measured dielectric spectrum is rather simple. It seems likely that the low frequency relaxation occurring around 10^6 Hz is a relaxation associated with the overall dipole of the individual mesogenic cores, which, being pair-wise correlated through the flexible spacer, do not orient independently. The stronger high frequency relaxation around 10^9 Hz, must be due to relaxation of the mesogenic dipolar ester groups around their local long molecular axes. Since these results are for the isotropic phase, the mesogenic axes are not ordered, but will adopt relative orientations determined by the conformational distribution in the isotropic phase.

In figures 2 (*a–c*), we present measurements of the real and imaginary parts of the permittivity for three temperatures in the nematic phase. The alignment is assumed to be approximately planar, but no bias field was applied. The results obtained at the lowest temperature (50°C), figure 2 (*c*), clearly show three relaxations, and the continuity of the Arrhenius plots over the full range of temperature give us confidence that the number and frequencies of the peaks for measurements at higher temperatures have been correctly identified.

In fact the data at all temperatures in the nematic phase can be fitted extremely well using equation (1), and assuming three relaxations designated ω_1, ω_2 and ω_3. As the temperature approaches the isotropic phase, the contributions from the two low frequency relaxations, ω_2 and ω_3, become small. This suggests that there is virtually no contribution of the total molecular dipole, and that only the internal high frequency reorientation of the ester groups is contributing to the dielectric response. It is important to note, however,

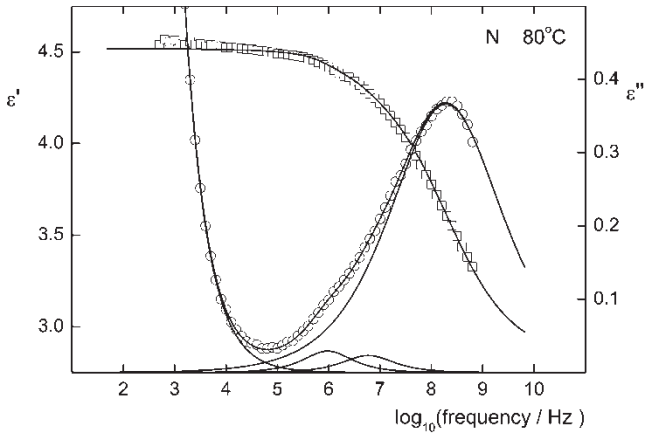

(*a*)

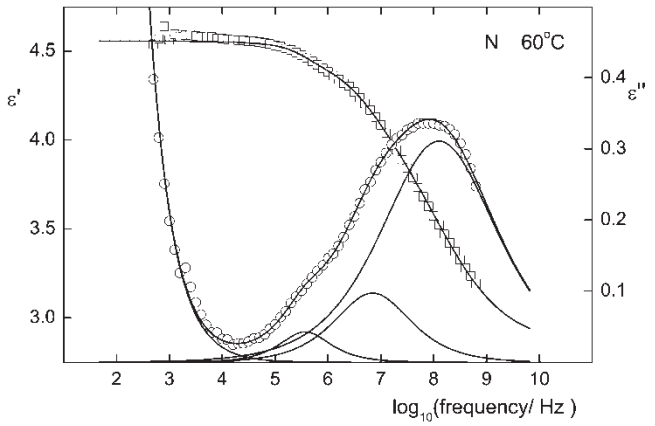

(*b*)

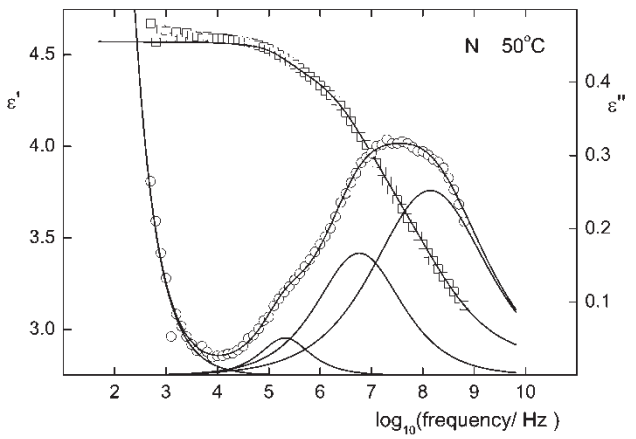

(*c*)

Figure 2. Complex dielectric permittivity vs logarithm of the frequency at (*a*) 80°C, (*b*) 60°C, (*c*) 50°C, in the nematic phase: □ real component; ○ imaginary component. The solid lines give the best fit to equation (1) with three modes (from high to low frequency): mode 1, mode 2, mode 3.

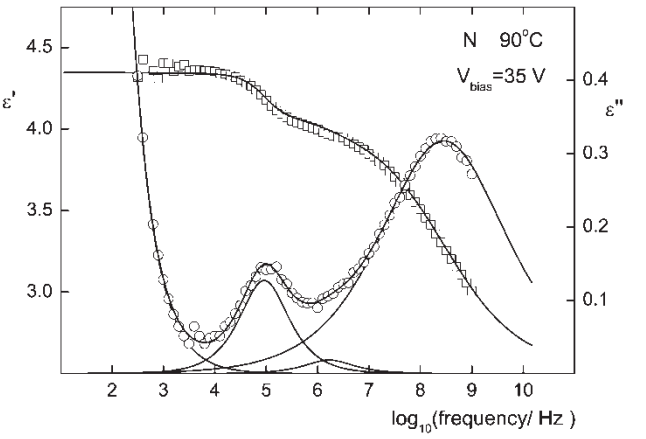

Figure 3. Complex dielectric permittivity vs logarithm of the frequency at 90°C in the nematic phase under a d.c. bias voltage: □ real component; ○ imaginary component. The solid lines give the best fit to equation (1) with three modes (from high to low frequency): mode 1, mode 2, mode 4.

that in the isotropic phase there is an increased contribution from another lower frequency relaxation. This is because, for a planar alignment in the nematic phase, there should be no contribution to the dielectric relaxation from an end-over-end reorientation mode of the total molecular dipole. Such a mode can contribute to the relaxation in the isotropic phase, since there is no longer any restriction on the molecular orientation. Application of a bias field to a planar aligned nematic sample of negative dielectric anisotropy should simply improve the planar alignment. However for the sample studied here, application of a bias field results in the appearance of a new relaxation at still lower frequency ω_4. This is illustrated in figure 3, where it is clear that the relaxation is due to the manifestation of a new mode.

Microscopic observations, see figure 4, confirmed that the appearance of the new mode was coincidental with the observation of electrohydrodynamic instabilities.

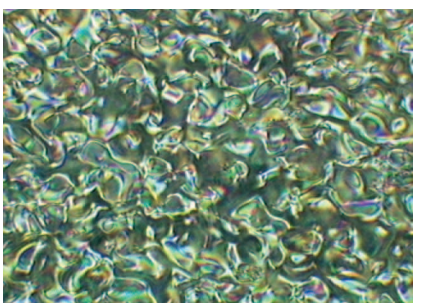

Figure 4. Electrohydrodynamic instabilities at 80°C in the nematic phase. Thickness = 25 μm, $V_{bias} = 5$ V.

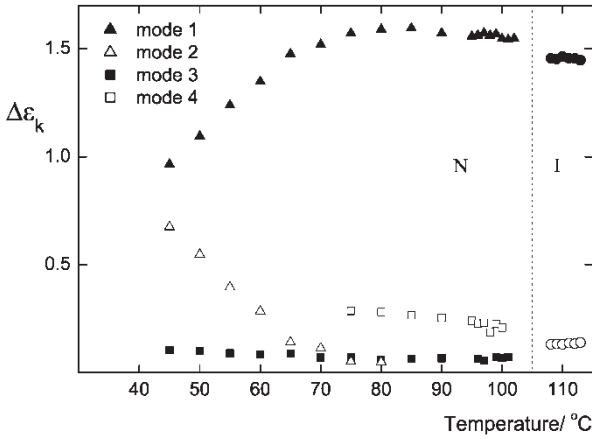

Figure 5. Dielectric strength of the relaxation modes vs temperature.

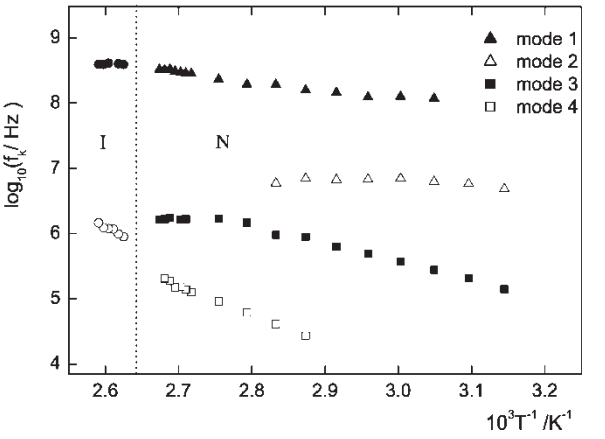

Figure 6. Arrhenius plot of the frequency of the relaxation modes.

Thus we propose that the electroconvection in the sample caused by the bias field allows us to observe the relaxation ω_4 due to the end-over-end reorientation of the molecular dipole as whole. This would normally contribute only to the parallel component of the permittivity, and so for materials of negative dielectric anisotropy is difficult to observe. It should be pointed out that the frequency of the relaxation that appears in the presence of a bias field applied to the nematic phase is similar to that expected by extrapolation of the low frequency relaxation from the isotropic phase.

The strengths of the relaxations, derived from fitting the measurements to equation (1) are given as a function of temperature in figure 5. It is noteworthy that the relaxation modes corresponding to ω_2 and ω_1 seem to be coupled, since over the temperature range 80 to 45°C the strength of relaxation mode ω_2 increases, while that of mode ω_1 decreases by corresponding amounts. Fitting parameters and activation energies for the relaxation processes are given in the table, and the logarithm of the relaxation frequencies are plotted as a function of inverse reciprocal temperature in figure 6.

Table. Fitting parameters and activation energies.

Mode	Activation energy/kJ mol^{-1}	Fitting parameter	
		α	β
Isotropic			
High frequency	–	0.5	1
Low frequency	~80	1	1
Nematic			
1	25	0.55	1
2	6	1[a]	1
3	53	1	1
4	84	1	1

[a] α decreases as T approaches T_g

5. Discussion

Two well separated relaxations can be identified in the dielectric spectrum for the isotropic phase of the laterally connected siloxane dimer. The high frequency mode ($\sim 3 \times 10^8$ Hz) has a very low activation energy, and a relatively high dielectric strength. The dimer contains three ester groups, each of which has a dipole component at right angles to the axes of the mesogenic groups; the high frequency mode may be attributed to intramolecular rotation of the ester groups. Given the flexible nature of the dimer, it must be assumed that changes in molecular shape do not significantly affect this relaxation mode. The low frequency relaxation observed in the isotropic phase has only a small strength, but a relatively high activation energy estimated to be in the region of 80 kJ mol^{-1}; there were insufficient experimental points in the isotropic phase to obtain a more accurate determination. This low frequency mode could be interpreted either in terms of the reorientation of the whole molecule, represented as an average over the contributing conformations [5] or, alternatively, in terms of the spacer correlated reorientation of the mesogenic cores of the dimer [11].

On lowering the temperature to the nematic phase, there is a qualitative change in the dielectric spectrum, and four relaxations are observed. Of these, three are present for the assumed planar alignment (i.e. that corresponding to the perpendicular component of the permittivity). The lowest frequency relaxation appears only in the presence of a bias electric field, and as explained above is assumed to be associated with the parallel component of the permittivity. In the spectra recorded for the planar alignment, there is a further qualitative change as the temperature is lowered below 80°C, such that the strength of the highest frequency mode ω_1 decreases, while that of the next highest

frequency mode ω_2 increases. We associate the highest frequency mode with independent rotations of the ester groups about the axes of the mesogenic units of the dimer, which also dominate the high frequency relaxation behaviour in the isotropic phase. We further believe that the mode ω_2, which becomes more apparent at lower temperatures in the nematic phase, is also due to relaxation of the net dipole of the ester groups, but this mode is precessional about the director axis. The activation energy for this process is initially very small, but as the temperature falls below 70°C the relaxation broadens, and the apparent activation energy increases, giving a strongly non-Arrhenius temperature dependence for the relaxation frequency. This behaviour suggests that the mode ω_2 is a co-operative one, in which the precessional motion of the dipoles associated with the terminal mesogenic groups of the dimer is coupled through the linking chain. As the temperature of the nematic phase falls, a glass transition is approached; the co-operative precessional mode becomes a collective mode, and moves to lower frequencies. This is to be contrasted with the behaviour of the fast internal rotation mode ω_1, the frequency of which is independent of temperature even at low temperatures. However as the temperature is lowered in the nematic phase, there is a reduction in the strength of the high frequency ω_1 mode, and a corresponding increase in the strength of the collective mode ω_2. Since we believe that ω_1 is due to an internal relaxation, then the loss of dielectric strength without change of frequency must be due to a reduction in the number of dipolar groups contributing to the ω_1 mode. A possible explanation is that at low temperatures only those ester groups which are disconnected from the linking chain are able to contribute to the high frequency ω_1 mode. As the temperature is lowered in the nematic phase, the co-operative precessional motion of the ester group dipoles attached to the linking chain becomes a collective mode ω_2. A comparison with polymer relaxations may be made if the ω_1 mode is identified as an Arrhenius β-relaxation, while the ω_2 process is an α-relaxation, which becomes non-Arrhenius at low temperatues.

The frequency and temperature behaviour of the mode ω_2 is illustrated in figure 7, where its development as a collective mode at low temperatures is clearly observed. The behaviour of other modes is also illustrated, but it is the mode ω_2 that dominates the dielectric response, especially at low temperatures.

There is a small contribution to the dielectric response of planar aligned samples from an activated mode ω_3, which is attributed to (correlated) precessional motion of the overall dipole of the mesogenic cores about the nematic director. At temperatures close

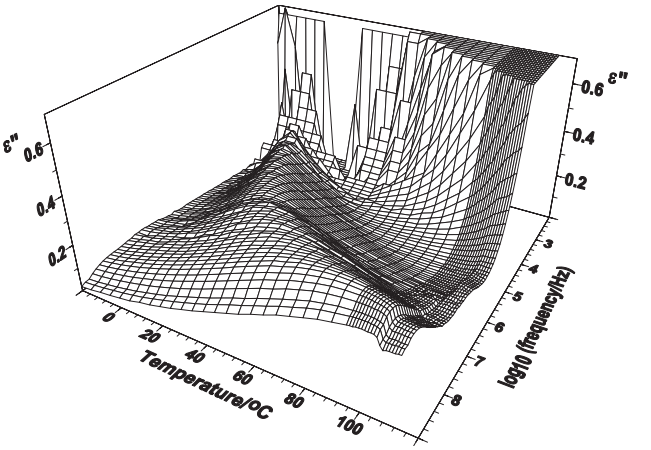

Figure 7. Three-dimensional plot of the dielectric losses vs temperature and logarithm of the frequency.

to the isotropic to nematic transition, the activation energy for this mode is close to zero. However as collective motion becomes important in the nematic phase, the motion becomes activated, with a relatively high activation energy for this mode. The strength of this mode decreases when a bias field is applied, and a new low frequency mode appears.

The lowest frequency mode ω_4 is observed only in the presence of a bias field, and has all the characteristics of a flip–flop relaxation of the overall molecular dipole, typical of most dipolar nematic liquid crystals. This mode contributes only to the parallel component of the dielectric permittivity, and so would not normally be detected for planar aligned samples. However the conduction alignment induced by the bias field allows the mode to be observed in our measurements. While the temperature dependence of the relaxation frequency can be accurately determined, the strength of the relaxation is not well defined, since the sample in a state of electrohydrodynamically induced turbulence is not uniformly aligned.

6. Conclusions

The introduction of internal flexibility into mesogenic molecules gives rise to additional mechanisms for the relaxation of dielectric polarization. Measurements reported in this paper, on the dielectric response of a laterally connected liquid crystal dimer, have revealed the existence of four separable relaxation processes in the nematic phase, and two in the isotropic phase. These have been identified with different relaxation modes for the dipolar groups in the molecule. Of particular interest is the mode labelled ω_2, which at high temperatures in the nematic phase behaves as a precessional mode characteristic of low molecular mass mesogens. However it seems that as the temperature is lowered in the nematic phase, the ester groups

contributing to this mode become coupled through the flexible linking chain, and a co-operative mode develops, which persists with a steadily increasing activation energy until the glass transition temperature is reached. Two features have emerged from our investigation of the dielectric properties of liquid crystal dimers. The first is that there are extra dielectric relaxations, which provide additional information on the molecular dynamics. The second is that with both laterally connected and terminally connected dimers, transfer of polarization between modes occurs as a function of temperature in the mesophase. This intramolecular transfer of polarization can be interpreted either in terms of a coupling between internal and external relaxation modes, or in principle equivalently as a change in average shape of the relaxing molecule. If changes of molecular shape can be programmed into a mesogen, they can provide an additional design tool to engineer the physical properties of liquid crystals.

This research was supported through the following programmes: EC Training and Mobility of Researchers Network, Contract No. FMRX CT97 0121; Universidad del Pais Vasco 9/UPV060.310-G16/98 and Spanish Government project C.I.C.Y.T. MAT 2000-1293-C02-02.

References

[1] Hardouin, F., Richard, H., and Achard, M. F., 1993, *Liq. Cryst.*, **14,** 971.
[2] Tournilhac, F., Bosio, L., Nicoud, J. F., and Simon, J., 1988, *Chem. Phys. Lett.*, **145,** 452.
[3] Imrie, C. T., and Luckhurst, G. R., 1998, in *Handbook of Liquid Crystals*, Vol. 2B, edited by, D. Demus, J. Goodby, G. W. Gray, H.-W. Spiess, and V. Vill (Weinheim: Wiley-VCH), p.801.
[4] Mehl, G. H., Thornton, A. J., and Goodby, J. W., 1999, *Mol. Cryst. liq. Cryst.*, **332,** 2965.
[5] Dunmur, D. A., Luckhurst, G. R., de la Fuente, M. R., Diez, S., and Peréz Jubindo, M. A., 2001, *J. chem. Phys.*, **115,** 8681.
[6] Photinos, D. J., Samulski, E. T., and Toriumi, H., 1992, *J. chem. Soc. Faraday Trans.*, **88,** 1875.
[7] Furuya, H., Okamoto, S., Abe, A., Petekidis, G., and Fytas, G., 1995, *J. phys. Chem.*, **99,** 6483.
[8] Serpi, H. S., and Photinos, D. J., 2000, *Mol. Cryst. liq. Cryst.*, **352,** 205.
[9] Kramer, L., and Pesch, W., 2001, in *Physical Properties of Liquid Crystals: Nematics*, edited by D. A. Dunmur, A. Fukuda, and G. R. Luckhurst (London: INSPEC), p.441.
[10] Tajber, L., Kocot, A., Vij, J. K., Merkel, K., Zalewska-Redak, J., Mehl, G. H., Elsasser, R., Goodby, J. W., and Veith, M., 2002, *Macromolecules*, **35,** 8601.
[11] Karahaliou, P. K., Photinos, D. J., and Dunmur, D. A. (to be published).